Neuron
Article

Diminished Schwann Cell Repair Responses Underlie Age-Associated Impaired Axonal Regeneration

Michio W. Painter,[1,2] Amanda Brosius Lutz,[3] Yung-Chih Cheng,[1] Alban Latremoliere,[1] Kelly Duong,[1] Christine M. Miller,[4,5] Sean Posada,[3] Enrique J. Cobos,[1] Alice X. Zhang,[1] Amy J. Wagers,[4,5,6] Leif A. Havton,[7] Ben Barres,[3] Takao Omura,[1] and Clifford J. Woolf[1,*]

[1]F.M. Kirby Neurobiology Center, Boston Children's Hospital and Department of Neurobiology, Harvard Medical School, Boston, MA 02115, USA
[2]Immunology Program, Harvard Medical School, Boston, MA 02115, USA
[3]Department of Neurobiology, Stanford University School of Medicine, Stanford, CA 94305, USA
[4]Department of Stem Cell and Regenerative Biology, Harvard University, Cambridge, MA 02138, USA
[5]Joslin Diabetes Center, Boston, MA 02215, USA
[6]Howard Hughes Medical Institute, Chevy Chase, MD 20815, USA
[7]Departments of Anesthesiology & Perioperative Care, Neurology and Anatomy & Neurobiology, University of California, Irvine, Irvine, CA 92697, USA
*Correspondence: clifford.woolf@childrens.harvard.edu
http://dx.doi.org/10.1016/j.neuron.2014.06.016

SUMMARY

The regenerative capacity of the peripheral nervous system declines with age. Why this occurs, however, is unknown. We demonstrate that 24-month-old mice exhibit an impairment of functional recovery after nerve injury compared to 2-month-old animals. We find no difference in the intrinsic growth capacity between aged and young sensory neurons in vitro or in their ability to activate growth-associated transcriptional programs after injury. Instead, using age-mismatched nerve transplants in vivo, we show that the extent of functional recovery depends on the age of the nerve graft, and not the age of the host. Molecular interrogation of the sciatic nerve reveals that aged Schwann cells (SCs) fail to rapidly activate a transcriptional repair program after injury. Functionally, aged SCs exhibit impaired dedifferentiation, myelin clearance, and macrophage recruitment. These results suggest that the age-associated decline in axonal regeneration results from diminished Schwann cell plasticity, leading to slower myelin clearance.

INTRODUCTION

Successful regeneration of the peripheral nervous system (PNS) requires the coordinated activity of several distinct yet interlocking systems. After axonal injury, neurons activate transcriptional "intrinsic growth" programs and begin extending new axons. Schwann cells (SCs) in the distal nerve undergo a rapid reprogramming process, dedifferentiating into nonmyelinating repair cells that secrete proregenerative factors, clear nonpermissive myelin, recruit macrophages, and create physical tracks onto which newly growing axons can navigate. Macrophages, in turn, enter the site of nerve injury from the circulation and help to complete clearance of myelin and axonal-derived debris, obstacles to regrowth. Remarkably, these complex intrinsic and extrinsic processes can lead to some restoration of function after peripheral nerve trauma.

As with most mammalian tissues, however, the regenerative capacity of the PNS declines with advancing age (Nagano, 1998; Pestronk et al., 1980; Tanaka and Webster, 1991; Vaughan, 1992; Verdú et al., 2000). In humans, an association between age and functional recovery has been pondered since at least World War II, and more recent clinical data quantify this correlation, such as after brachial plexus injury or median nerve transection (Woodhall, 1956; Nagano, 1998; Lundborg and Rosén, 2001). In addition, broader defects of the aging PNS have also been widely noted. For example, it is estimated that nearly one in three persons over the age of 65 suffers from some form of peripheral neuropathy, and the underlying cause in the majority of these instances is considered idiopathic (Cho et al., 2006). Thus, understanding how the PNS changes with normal aging is clinically important.

To some degree, the clinical associations between age and the extent of neuronal regeneration have been recapitulated in animal models. While not addressing functional recovery directly, an age-associated impairment of axonal regeneration can be detected in both mice and rats through histological assessments (Verdú et al., 2000). More recently, studies have shown similar phenomena in both zebrafish and the nematode *C. elegans* (Graciarena et al., 2014). Interestingly, the developmental decline in axonal regeneration found in the nematode *C. elegans* is the result of neuronal intrinsic alterations (Zou et al., 2013). In the case of mammals, however, to what degree age-associated impairment of axonal regeneration represents neuronal intrinsic alterations versus environmental perturbations remains an open and critical question, with significantly different therapeutic implications.

In this study, we used 24- and 2-month-old mice along with standard models of peripheral nerve injury to assess the potential contributions of neurons, immune cells, and peripheral glia to

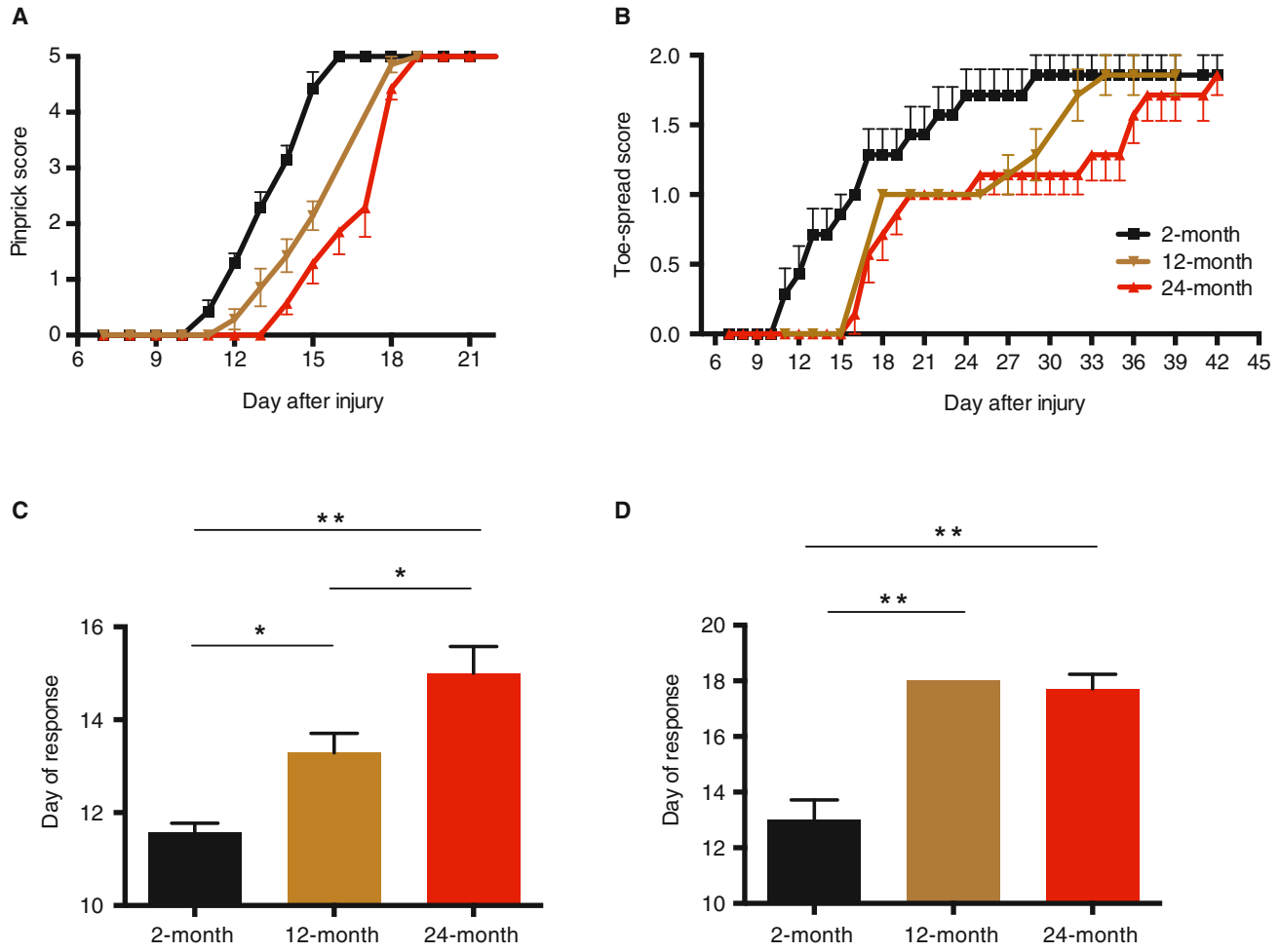

Figure 1. Progressive, Age-Dependent Deficit in Peripheral Nerve Regeneration

Cohorts of 2-, 12-, and 24-month-old mice were subjected to sciatic nerve crush injury and restoration of sensory (A) and motor (B) function, assayed through pinprick and toe-spreading assays, respectively. The first day in which a positive sensory (C) or motor (D) behavioral response occurred was also recorded. *$p < 0.05$; **$p < 0.01$ in one-way ANOVA with Bonferroni multiple comparisons test. Full statistics found in Supplemental Information. Mean ± SEM, n = 7–8 mice per cohort.

the aging phenotype. Our results demonstrate that extrinsic factors are sufficient to rejuvenate the age-associated decline in mammalian axonal regeneration, and broadly reveal how SC function and its response to axonal injury alters during normal aging, resulting in slower dedifferentiation and myelin clearance.

RESULTS

Although previous studies have established in rodents that fewer axons regenerate after injury in aged animals, it is unclear how this might translate into functional recovery, a more meaningful clinical parameter. We thus first sought to establish whether aging impaired functional recovery in mice after nerve injury. To accomplish this, we performed a sciatic nerve crush injury (a model in which full recovery is expected [Ma et al., 2011]) on cohorts of 2-, 12-, and 24-month-old C57BL/6 mice, and assayed their sensory and motor functional recovery over time, using behavioral-based assays (see Experimental Procedures). In young mice, full sensory recovery is achieved approximately 15 days after injury, while motor function is restored by day 30, reflecting the short distances and consistent with axon growth of 1–2 mm per day, similar to that found in humans. Aging, however, produces a progressive defect in the onset and time to restoration of motor and sensory function in the mice, with an approximately 3–4 day (~29%) difference in maximum recovery between young and aged animals for sensory function and a 9–10 day delay (~44%) for recovery of motor function (Figures 1A and 1B). Middle-aged animals (12 months) show an intermediate phenotype, indicating that age-dependent slowing of functional recovery is acquired gradually throughout life. Interestingly, the kinetics of these behavioral data suggest that the prominent effect of age is not a slower overall rate of regeneration, but instead a marked delay in the initiation of regeneration in the first place (Figures 1C and 1D).

What is responsible for this defect? Because axonal regeneration in mammals is driven by the transcriptional activation of neuronal intrinsic growth programs after injury (Chen et al., 2007; Seijffers et al., 2007), it has been suggested that the

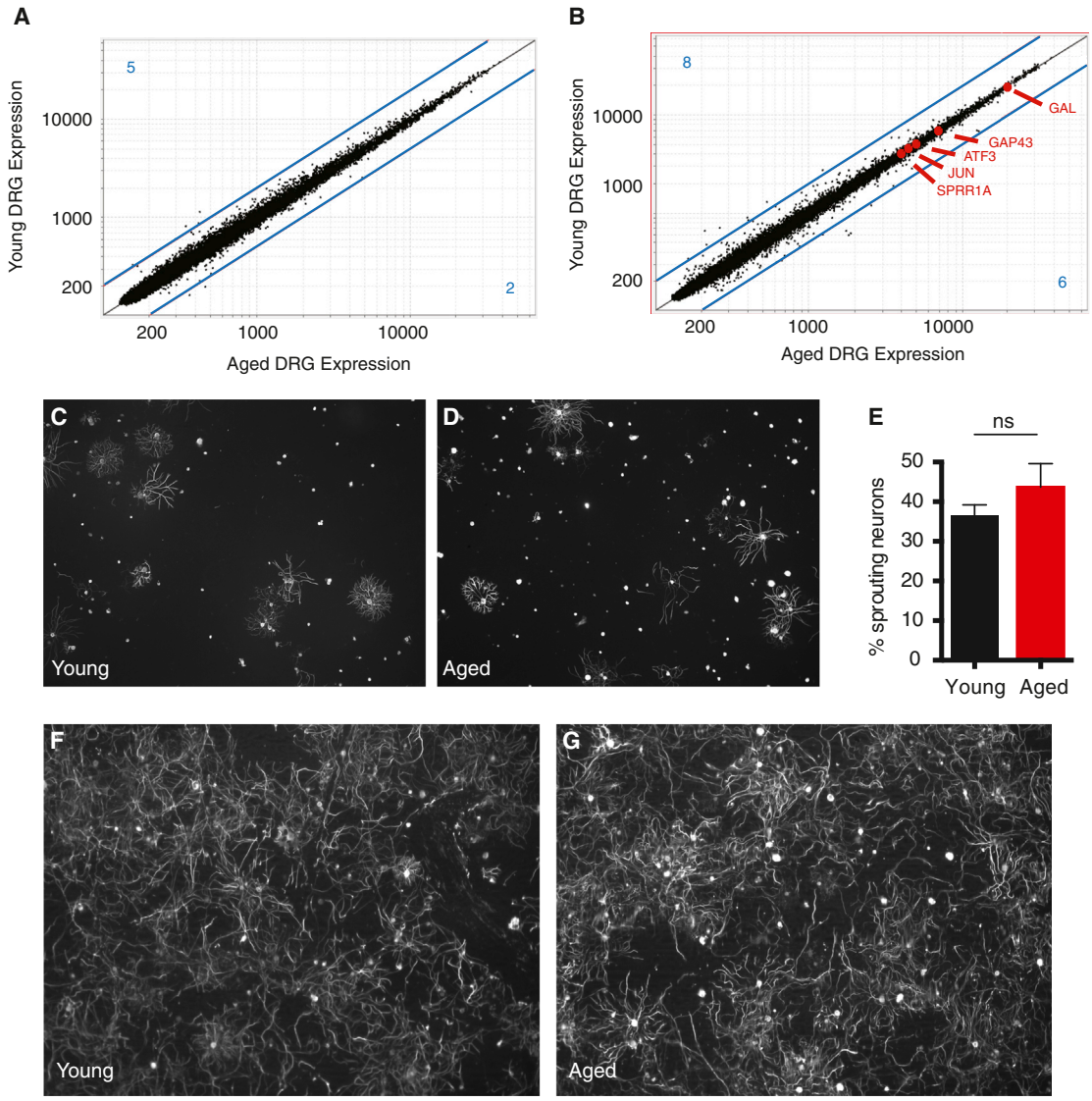

Figure 2. Neuronal Intrinsic Growth Responses to Injury Remain Robust throughout Life

(A and B) Microarray data from DRG neurons. Expression of young DRGs versus expression of aged DRGs in (A) naive conditions and (B) 4 days after nerve crush injury. Known markers of regeneration are highlighted in red. Lines in blue represent fold change = 2; blue numbers in each corner represent the number of genes over- or underexpressed by more than 2 fold.

(C–G) In vitro neurite outgrowth assays of DRG sensory neurons. Sensory neurons from naive young (C) or aged (D) DRGs from aged or young animals were purified and cultured for 17 hr and neurite outgrowth measured with NeuroMath (E). Mean ± SEM, n = 3 independent experiments per group, NS = not significant with unpaired t test. DRG sensory neurons from young (F) or aged (G) animals were purified 4 days after nerve injury and cultured for 12 hr, revealing robust preconditioning responses.

age-related decline in regeneration may be the consequence of a diminished intrinsic growth potential of aged neurons (Pestronk et al., 1980). Unexpectedly, however, we find by transcriptional profiling of young (2-month) and aged (24-month) dorsal root ganglias (DRGs), both before and after nerve injury, extremely comparable gene-expression signatures, with similar levels of injury-induced transcriptional activation between young and old ages (Figures 2A, 2B, and S1A available online). After nerve injury, over 250 genes in the DRG are up- or downregulated greater than 2-fold compared to naive controls (Figure S1B). Among these, only 14 are differentially expressed (>2-fold) between young and aged animals. Many of these age-variant transcripts are also deregulated in naive (uninjured) conditions, implying they are part of a "background" aging signature and not specific to nerve injury (Table S1). Important "regeneration-associated genes" such as *ATF3*, *GAP43*, and *Sprr1a* were not differentially expressed between young and aged DRGs (Figure 2B) (Bonilla et al., 2002; Chong et al., 1994; Seijffers et al., 2007). As predicted from the transcriptional data, in vitro neurite outgrowth assays using dissociated neurons revealed

comparable growth activity regardless of age, in both naive and preconditioned DRG sensory neurons, confirming no deficit with age in the degree of intrinsic neuronal growth induced by injury (Figures 2C–2G). These experiments strongly argue that a mechanism extrinsic to neurons moderates the regenerative potential of aging DRG neurons in vivo.

As such, we hypothesized that allowing "aged" axons to regenerate into a "youthful" environment might enhance functional recovery in aged animals. Conversely, we conjectured that forcing young axons to regenerate into an "aged" environment would result in impaired recovery. To test this, we harvested 1 cm segments of sciatic nerve from either aged or young animals and directly sutured them onto the two cut ends of transected sciatic nerves of either old or young animals. In this way, axons from the host animal must regenerate through a 1 cm segment of either age-matched or age-mismatched nerve tissue before reaching the distal end of the nerve en route to their targets in the skin (Figure 3A). We assessed sensory functional recovery to monitor regeneration. Because transection/resuture injuries are more severe than crush injuries, motor recovery of plantar muscles in the foot is not obtained, and functional sensory recovery takes much longer (Ma et al., 2011). Strikingly, we observed that functional recovery was enhanced in aged animals receiving young nerve grafts such that it now resembled that found in young animals receiving young nerve grafts (Figure 3B). Reciprocally, young animals receiving aged nerve grafts showed slower functional recovery, similar to aged animals receiving aged nerve grafts (Figure 3B).

We further quantified the extent of axonal regeneration in an age-mismatched system. To accomplish this, we used a different nerve graft strategy in which either young or old 1-cm-long pieces of sciatic nerve were sutured onto the proximal cut end nerves of Thy1 YFP+ young host animals (aged transgenic mice were not available for the reciprocal experiment) (Figure 3C). Thy1 YFP+ mice were chosen to enable visualization of regenerating fibers in the graft. After 1 week, the number of YFP+ axons growing into either young or aged donor tissue was quantified histologically. Forcing young axons to regenerate into an aged environment, as opposed to a young one, severely impaired the extent and length of growth, with reduced numbers of axons at every distance from the site of the graft (Figures 3D and 3E).

Given the age-dependent ability of factors extrinsic to the injured neurons to modulate axonal growth, we next sought to identify what age-associated changes occur within the sciatic nerve environment. To this end, transcriptional profiling of young and aged nerves distal to a sciatic nerve ligation (to prevent regenerating axons from contaminating samples) revealed widespread age-related alterations (Figures 4A–4C, S2A, and S2B; Tables S2 and S3). From a global perspective, gene pathway analyses of differentially represented transcripts between young and aged nerves showed several significantly enriched pathways, using the Kyoto Encyclopedia of Genes and Genomes (KEGG) and Gene Ontology (GO) databases (Figures 4A, 4B, S3A, and S3B). In young nerves after injury, this included prominent overrepresentation of genes associated with "cell cycle," "DNA replication," and the "extracellular matrix," while genes associated with the "inflammatory response" were among the pathways relatively enriched in old nerves (Figures 4A and 4B). Several pathways are also enriched in young nerves in naive conditions, such as genes associated with the "extracellular matrix" and "lipid biosynthesis" (Figures S3A and S3B). This analysis suggests that a greater degree of cell proliferation may occur in young than aged nerves distal to an injury.

The specific age-associated alterations can be seen prominently by the number of transcripts that deviate from the Y = X parity line in the fold change versus fold change plot, indicating that hundreds of genes up- or downregulated after injury in the young are not equally regulated in aged nerves. Strikingly, we found that many of these genes are associated with a "repair program" in SCs activated after injury (Figure 4C; Table S3). After nerve injury, SCs undergo a phenotypic reprogramming process whereby they downregulate their myelinating phenotype, rapidly divide, and acquire a nonmyelinating "repair cell" phenotype critical for the development of a growth-permissive environment within the nerve that facilitates regeneration (Arthur-Farraj et al., 2012; Mirsky et al., 2008).

We observed a prominent age-related deregulation of genes encoding key repair cell functions. Genes downregulated in aged nerves relative to young ones after injury included those associated with growth factors (*BTC*, *NGFR*, *BDNF*) and mitosis (e.g., *KIF2C*, *PBK*, *BIRC5*, *CDC20*) (Figure 4C; Table S3). Likewise, genes associated with myelin production (e.g., *PMP2*, *MPZ*, *MAL*, *EGR2*) were relatively overexpressed in lesioned aged animals, implying an impaired ability to downregulate their myelinating phenotype after injury (Figure 4C).

Recently, the transcription factor c-Jun was identified as a "master regulator" of the SC repair phenotype after nerve injury, and SC-specific ablation of *c-Jun* results in severely impaired functional recovery (Arthur-Farraj et al., 2012). Interestingly, we noticed marked similarities between the transcriptional profiles of injured aged nerves and genes altered in mice lacking c-Jun expression in SCs after injury (e.g., *MPZ*, *CDH1*, *SEMA4F*), suggesting that genes under control of c-Jun were altered in aged animals (Arthur-Farraj et al., 2012). Strikingly, western blot analysis demonstrated that the regulation of c-Jun protein was significantly different in the nerves of aged compared with young animals immediately after injury (Figures 4D and 4E). The initial burst of c-Jun expression found in the nerves of young animals 1 day after injury was approximately 5-fold higher than that in aged animals (Figure 4E). ERK and JNK, two upstream kinase pathways of c-Jun, were unaltered in aged sciatic nerves after injury (Figure S4).

If, as suggested by these data, SC dedifferentiation and repair cell functions are impaired with aging, one would predict functional consequences in the SCs, and more generally, for Wallerian degeneration in the nerve. To test this, we first performed toluidine blue staining and electron microscopy examination of distal sections of young and aged sciatic nerves. These revealed stark differences in Wallerian degeneration. By 3 days after a nerve crush injury in young mice, axons in the nerve distal to the injury have degenerated and been cleared, and the myelin sheaths surrounding the axons have also degenerated, leaving the nerve landscape largely empty of any organized structure (Figures 5A and 5C). In complete contrast, however, axons in the distal nerve of aged animals are at a less developed state

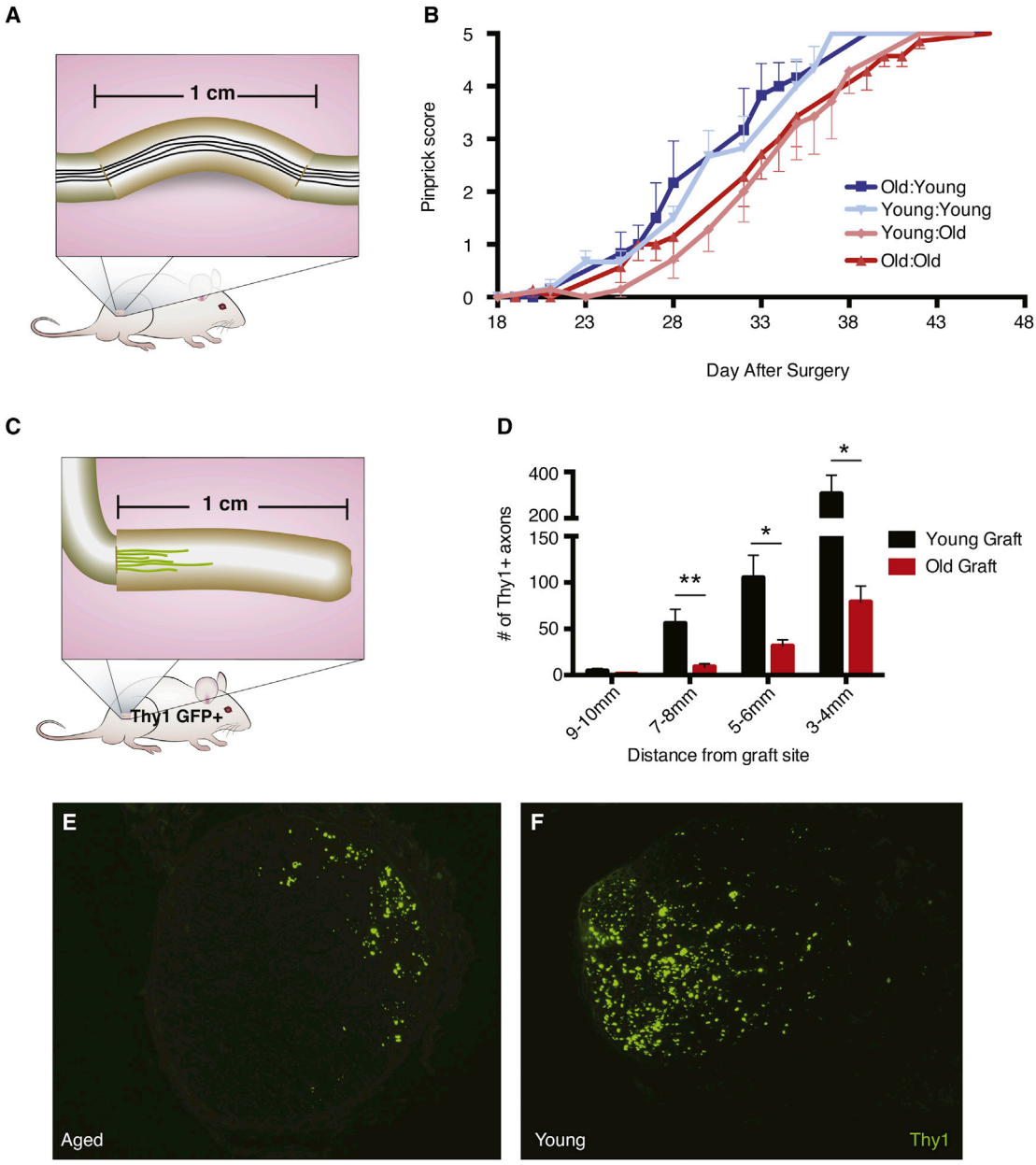

Figure 3. Neuronal-Extrinsic Factors Are Sufficient to Recapitulate or Rejuvenate the Phenotype

(A) Schematic of nerve graft strategy. Segments 1 cm long from young or aged animals were sutured into the nerves of either young or aged host animals and restoration of sensory recovery assayed as in Figure 1.

(B) Time course of sensory recovery as measured by pinprick score.

(C and D) (C) Schematic of Thy1 YFP+ graft strategy. Segments 1 cm long of sciatic nerves from either aged or young mice were sutured onto the sciatic nerves of young Thy1 YFP+ host animals and nerves analyzed histologically after 7 days (D). Representative images of YFP+ axons in the donor aged and young nerve grafts 5 mm distal to the site of suture.

(E) Quantification of the number of YFP+ fibers at each specified distance from the suture site. Axon counts were quantified using ImageJ. Mean ± SEM is plotted, n = 7 mice per group (one mouse with counts greater than 3 SD from the mean was removed from the data set). Stats: interaction age × graft distance; $p < 0.01$, two-way ANOVA; $F(3, 48) = 5$. *$p < 0.05$, **$p < 0.01$ with multiple t test, Holm-Sidak correction.

of degeneration and clearance, and more starkly, most myelin sheaths remain intact (Figures 5B and 5D). Quantification of axons with intact myelin sheaths shows approximately four times the number remaining in aged, as opposed to young, animals (Figure 5E). These data are consistent with previous histological studies in rodents, and quantify the aberrant delayed state of early Wallerian degeneration in aged animals (Vaughan, 1992; Verdú et al., 2000).

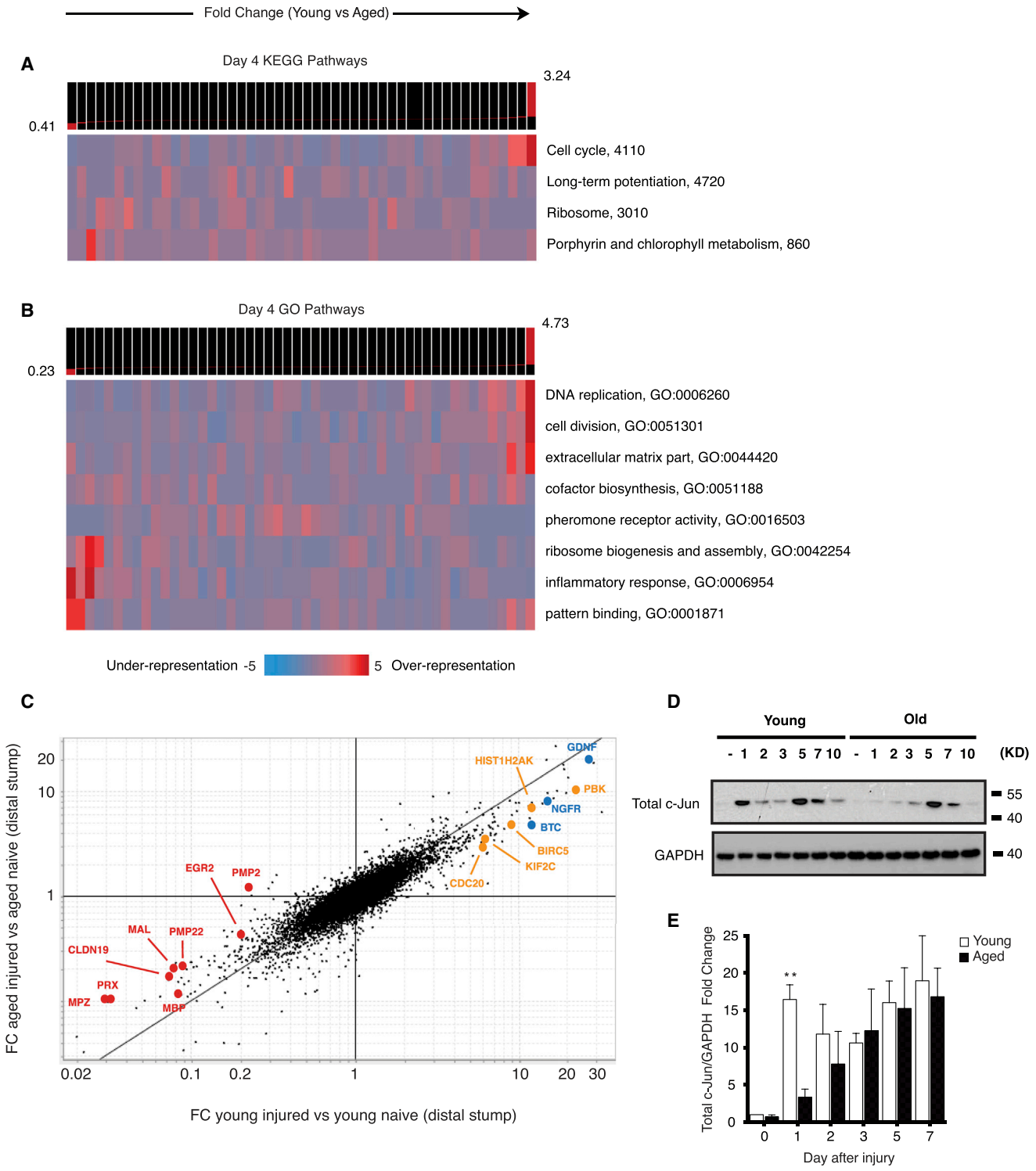

Figure 4. Acquisition of Repair Cell Phenotype Is Impaired in Aged Schwann Cells

(A and B) Significantly overrepresented gene pathways from KEGG (A) and GO (B) databases. Columns represent groups of genes according to their fold change difference in young versus aged sciatic nerves 4 days after crush injury. Columns to the left contain genes more overexpressed in old, whereas columns to the right contain genes more overexpressed in young. Heatmap depicts the pattern of expression of pathways across the groups of differentially expressed genes (see Goodarzi et al., 2009).

(C) Expression data from the distal nerve stump of aged and young animals after nerve transection/ligation injury. x axis represents fold change of young injured against young naive transcripts. y axis is fold change of aged injured against aged naive transcripts. Transcripts along the black y = x line represent

(legend continued on next page)

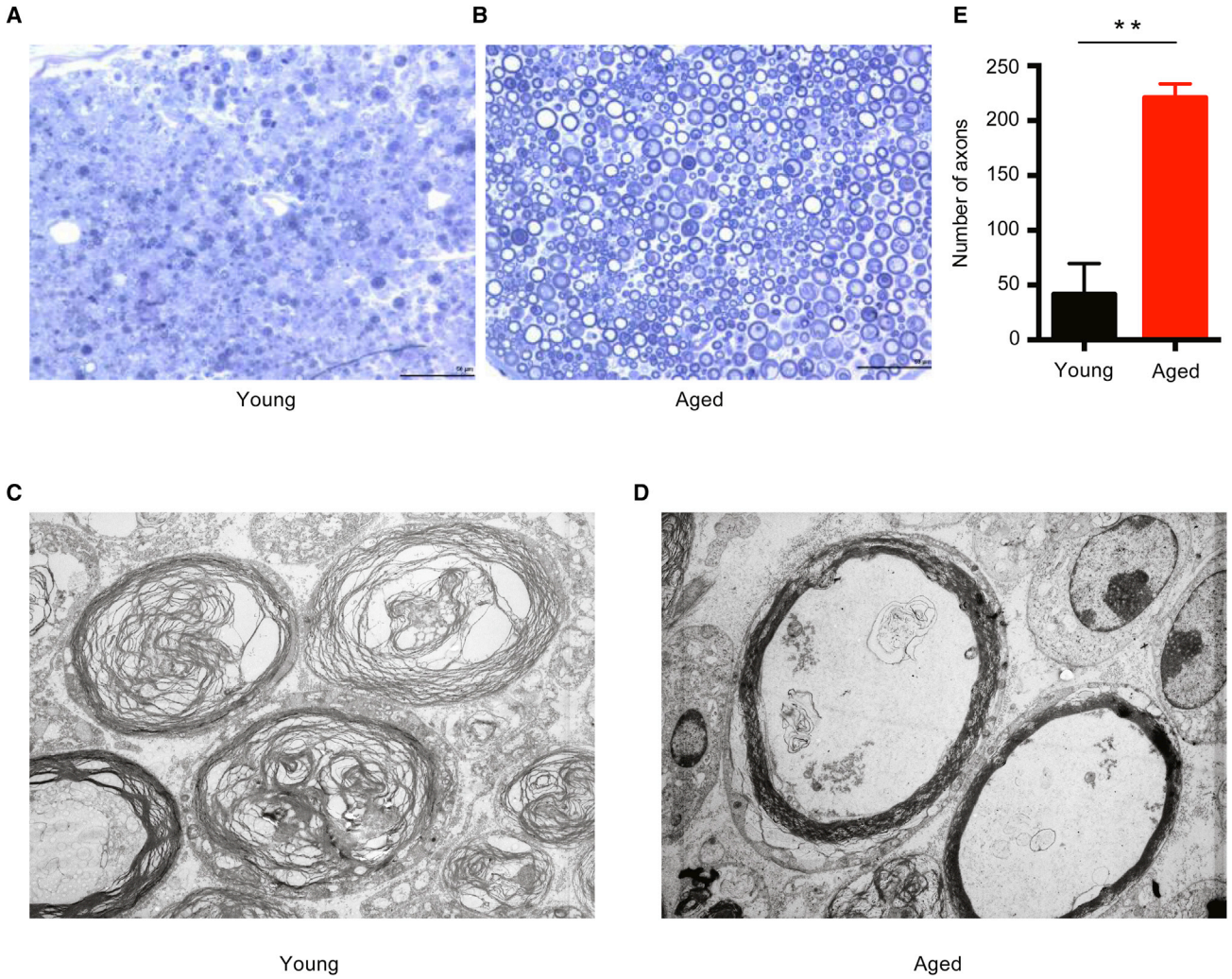

Figure 5. Wallerian Degeneration Is Disrupted in Aged Animals

(A–D) Toluidine blue staining of distal nerve sciatic sections 3 days after crush injury in young (A) and aged (B) animals. Electron microscopic images of same distal nerve sections from young (C) and aged (D) animals.

(E) Quantification of the number of intact myelin sheaths in aged and young nerves from toluidine blue staining. n = 4. **$p < 0.01$ with unpaired t test. Scale bar, 50 μm.

We next directly addressed if age affected SC function and repair responses after nerve injury. As expected, expression of p75, an induced marker for the repair cell phenotype, was delayed in aged SCs after sciatic nerve crush injury compared to young controls. In young animals, ~65% of S100+ SCs were positive for p75 3 days after nerve injury (Figures 6A, 7A, and 7B). S100 is an SC marker constitutively present in intact and dedifferentiated SCs. In aged animals, however, p75 reactivity was observed in only ~16% of S100+ SCs.

Repair SCs play several key roles to promote axonal regeneration and Wallerian degeneration. For example, macrophage recruitment into the degenerating nerve depends upon factors secreted by dedifferentiated SCs (Napoli et al., 2012). We thus measured macrophage recruitment into the degenerating nerve by tracking the expression of CD68, a standard marker for activated macrophages, over time. This revealed a markedly delayed recruitment of CD68+ macrophages after injury in aged animals of up to 7 days (Figures 7C and 7D). This delay in immune

equal up- or downregulation after injury compared to naive. Red = myelin-associated genes; blue = growth factors-associated; orange = mitosis-associated.

(D) Representative western blot analysis of total c-Jun in sciatic nerves after nerve injury.

(E) Summary of western blot analyses of c-Jun regulation in young and aged nerves (distal to the site of injury) after nerve injury. n = 3 biological replicates for all time points except day 7, where n = 2. **$p < 0.01$ with multiple t tests, Holm-Sidak correction.

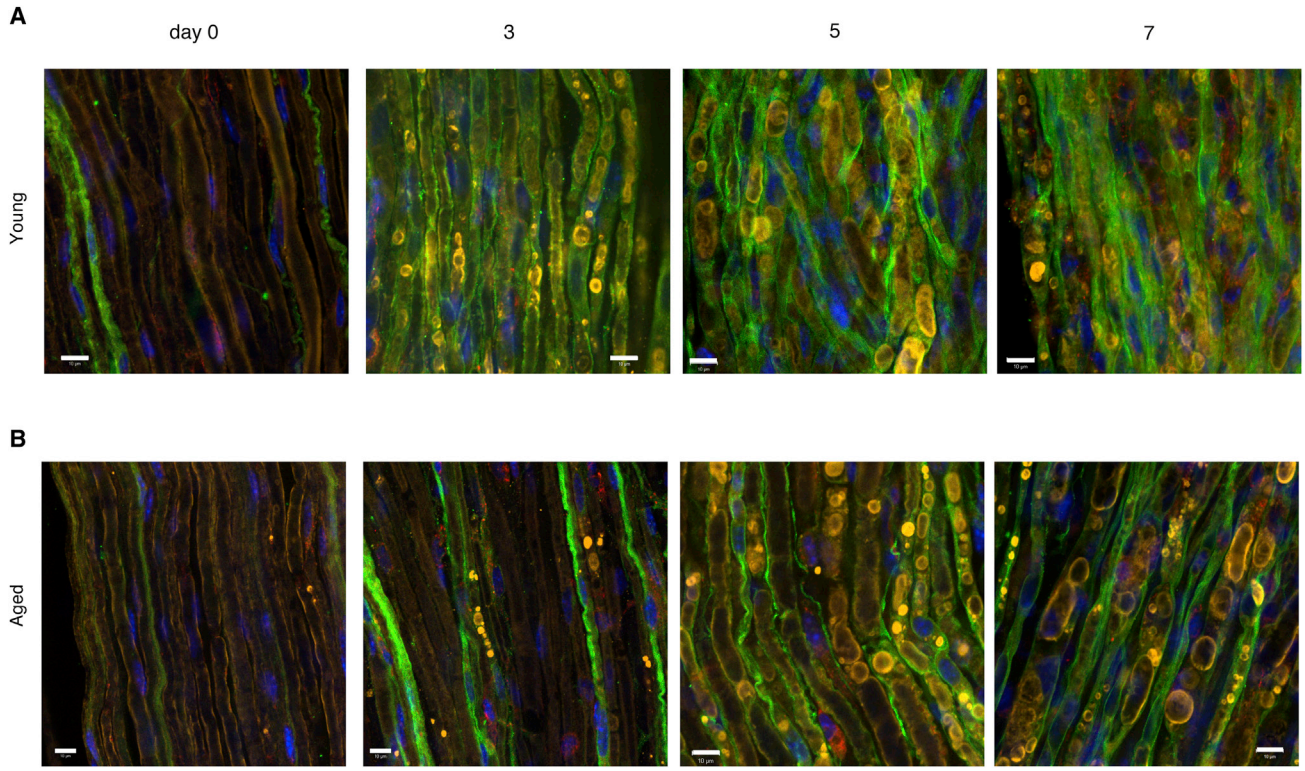

Figure 6. Aged Schwann Cell Injury Responses Are Delayed

Representative confocal images of sciatic nerves from young (A) and aged (B) animals at days 0, 3, 5, and 7 after nerve crush injury. Sections were stained with p75 (green), MBP (yellow), and Lamp-1 (red). Note strong colocalization between myelin and SCs at all time points observed. Scale bar, 10 μm.

cell recruitment is unlikely to be the result of a defect intrinsic to aged immune cells because heterochronic parabiosis, which provides aged animals with access to young hematopoietic cells, failed to rescue the aging phenotype (Figures S5A–S5F). This model successfully enhances remyelination in the CNS in a macrophage-dependent manner (Ruckh et al., 2012), and immune cell chimerism was detected in both the spleens and sciatic nerves of conjoined animals after nerve injury (Figures S5B–S5D).

Another critical downstream function of SCs after injury is the physical fragmentation of their myelin sheaths followed by intracellular degradation of myelin proteins and lipids. Myelin is an inhibitory substrate for axon growth, and it is thus essential that myelin debris is cleared from the distal injury site before regeneration can occur (McKerracher et al., 1994). SCs from aged mice showed a deficit in their ability to initiate myelin clearance during early time points after injury, in parallel with the delay in expression of p75 (Figures 7E and 7F). Dense MBP-positive myelin accumulations were colocalized within p75-positive (dedifferentiated) SCs soon after injury in young nerves, but not in p75-positive aged SCs (Figures 6A and 6B). The defect can be clearly seen from myelin staining in distal segments of the sciatic nerve after crush injury, where 3 days after injury to young nerves, SCs show large, bright, MBP-positive accumulation of fragmented myelin, indicating that myelin breakdown is underway, while in aged animals most MBP staining is evenly distributed in continuous sheaths, similar to intact nerves (Figures 7E and 7F).

The SC-mediated mechanism of intracellular myelin degradation is believed to depend on SC phagocytosis of extracellular myelin debris (Brosius Lutz and Barres, 2014). To directly address cell-intrinsic SC phagocytosis, we purified populations of SCs from young and aged sciatic nerves and cultured them in the presence of labeled myelin (Figure 7G). Quantification of the amount of myelin contained within SCs using fluorescence-activated cell sorting revealed 35% less phagocytosis of myelin in aged versus young SCs (Figure 7H). This defect was not the result of reduced viability of aged SCs (Figure 7I). Thus, aged SCs exhibit a reduced capacity for myelin breakdown and clearance in vitro and in vivo.

DISCUSSION

We have found that aging introduces a progressive decline in the initiation of axonal regeneration after injury in mammals. This age-dependent slowing in regenerative potential may contribute to the suboptimal clinical outcomes reported after nerve trauma in elderly individuals (Nagano, 1998; Lundborg and Rosén, 2001).

Our data also demonstrate that the regenerative capacity of the aging mammalian PNS is not limited by diminished neuronal growth responses, but is instead profoundly influenced by

extrinsic factors in the surrounding tissue. We found that neuronal intrinsic growth responses are unaltered with normal aging and that aged neurons can be fully "primed" to regenerate after an axonal injury supported by an undiminished injury-induced transcriptional change. This notion is consistent with recently published data demonstrating that the rate of axonal regeneration does not differ between young and aged mice in vivo (Kang and Lichtman, 2013). We further demonstrated that the ectopic introduction of aged tissue impeded regeneration in young, healthy mice, whereas grafting of young tissue enabled aged neurons to express a robust repair potential. These observations indicate that deficient axonal regeneration in aged animals arises from a dominant extrinsic inhibition of neuronal outgrowth by the aged microenvironment, and suggest that functional recovery after axotomy may be enhanced throughout life via neuron-extrinsic mechanisms.

Our analysis demonstrates that SC injury responses are substantially altered in aged animals, a defect we suggest is due to a failure of aged SCs to effectively activate an appropriate transcriptional repair response after axonal denervation. Although our studies were limited to C57/BL mice, their congruence with rat and human observations indicates that the phenomena described here are not likely to be restricted to this strain, but the strain dependence of this phenotype will need to be formally tested. Our data implicate aged SCs as key mediators of age-dependent inhibition of axon regeneration in the PNS. Although it remains to be determined whether the altered SC responses of aged animals result entirely from intrinsic defects (such as age-acquired DNA damage) or whether this represents a failure in an upstream signaling cascade initiated by a change in the distal cut axons leading to delayed c-Jun expression, it is clear that the failure of aged SCs to efficiently acquire a repair phenotype after nerve injury impinges on axonal regeneration. In the future, it will be of great interest to determine both the exact cause for these alterations in the SC compartment and whether they also contribute to other age-associated disorders of the PNS, such as idiopathic age-related peripheral neuropathy.

In terms of what specific SC defects impair the initiation of axonal regeneration, it is probable that inefficient SC dedifferentiation in aged animals may result in a variety of downstream consequences that could impair axonal growth. For example, as macrophages are required for proper axonal regeneration, the delay in macrophage recruitment we observed could contribute to the aging phenotype (Barrette et al., 2008). In addition, as seen from our profiling studies, in the aging nerve environment there is less growth factor production after injury. A distinct SC-related defect that likely impedes optimal axonal growth was that aged SCs have a markedly reduced capacity for myelin clearance, a critical component for establishing the regeneration-enabling environment of the injured PNS. Moreover, our data highlight the myelin clearance function of SCs early during the course of Wallerian degeneration, a role that has perhaps been underappreciated compared to their macrophage counterparts, which operate later, indeed at a time when most myelin is already cleared in young nerves. The mechanism of myelin breakdown by SCs is then an area requiring urgent future effort (Brosius Lutz and Barres, 2014).

SCs are potentially unique among adult, differentiated cells in that after injury they undergo a phenotypic reprogramming process that resembles transdifferentiation (Arthur-Farraj et al., 2012) and in this way acquire a dedifferentiated, highly proliferative, almost stem cell-like state. Given the well-known alterations that occur in stem cell compartments during normal aging, it is perhaps not surprising that SCs, which undergo major transcriptional and phenotypic changes after injury, may be relatively vulnerable to age-acquired alterations. Glial cells in the CNS also exhibit an age-associated decline in function. For example, the differentiation potential of oligodendrocyte progenitor cells declines with age, resulting in decreased myelination (Shen et al., 2008). Unlike what we have observed with SCs, however, this diminished function in CNS glia results in part from extrinsic signaling via hematopoietic cells (Ruckh et al., 2012).

Finally, our data may have bearing on therapeutic strategies for promoting neural repair in aged patients, where replication of a youthful extrinsic environment may be conducive to greater recovery. Although rare, limb transplants are now successfully performed, and our work would suggest that the age of the donor may influence outcomes more than that of the host.

EXPERIMENTAL PROCEDURES

Mice

Young (8- to 12-week-old) and aged (24- to 26-month-old) C57/BL6 mice were obtained from Charles River and the National Institute of Aging (NIA), respectively. Thy1 YFP+ animals were bred in house, originally obtained from Jackson Laboratory, line #003709. Animals were housed and handled in accordance with protocols approved by the Administrative Panel on Laboratory Animal Care (APLAC) of Stanford University or in full accordance with the IACUC guidelines of Children's Hospital Boston.

Sciatic Nerve Crush

All surgical experiments were performed under 2.5% isoflurane on either young-adult mice (8–12 weeks old) or aged mice (24–26 months old). Sciatic nerve crush injury was performed as previously described (Ma et al., 2011). Briefly, the sciatic nerve was exposed at midthigh level on the left side of the animal and crushed with smooth forceps for 30 s. For experiments involving Schwann cells (Figure 3), mice were anesthetized using isoflurane. Upper thigh was shaved and sterilized using isopropanol. A 1 cm incision was made using a scalpel, and nerve was visualized via blunt dissection using forceps. The left sciatic nerve was crushed at midthigh for 5 s using forceps marked with sterile graphite to mark the crush site. Carprofen (5 mg/kg subcutaneous) was administered for analgesia.

Sciatic Nerve Graft

For Thy1 experiments, 1-cm-long segments of the sciatic nerve (from midthigh level to the site of trifurcation) from either young or aged animals were acutely harvested and grafted using 10-0 nylon sutures onto the sciatic nerve just below the sciatic notch of 8-week-old Thy1 YFP mice. These nerves were only sutured at the proximal site, and the distal side was left as a free ending. For nerve graft studies involving behavioral assessments, 3 mm of the sciatic nerve was removed from the host mice and was replaced with a 1-cm-long sciatic nerve graft of either young or aged animals. The proximal and distal ends were sutured with 10-0 nylon.

Assessment of Sensory Recovery Using a Pinprick Assay

Pinprick assay was performed as described previously (Ma et al., 2011). Briefly, mice were habituated on wire mesh cages for 30 min, until calm, and then tested for pain responses on the hind paw using a small insect needle. All experiments were repeated by at least two separate investigators. In the case of nerve graft studies, experiments were conducted blinded to the age

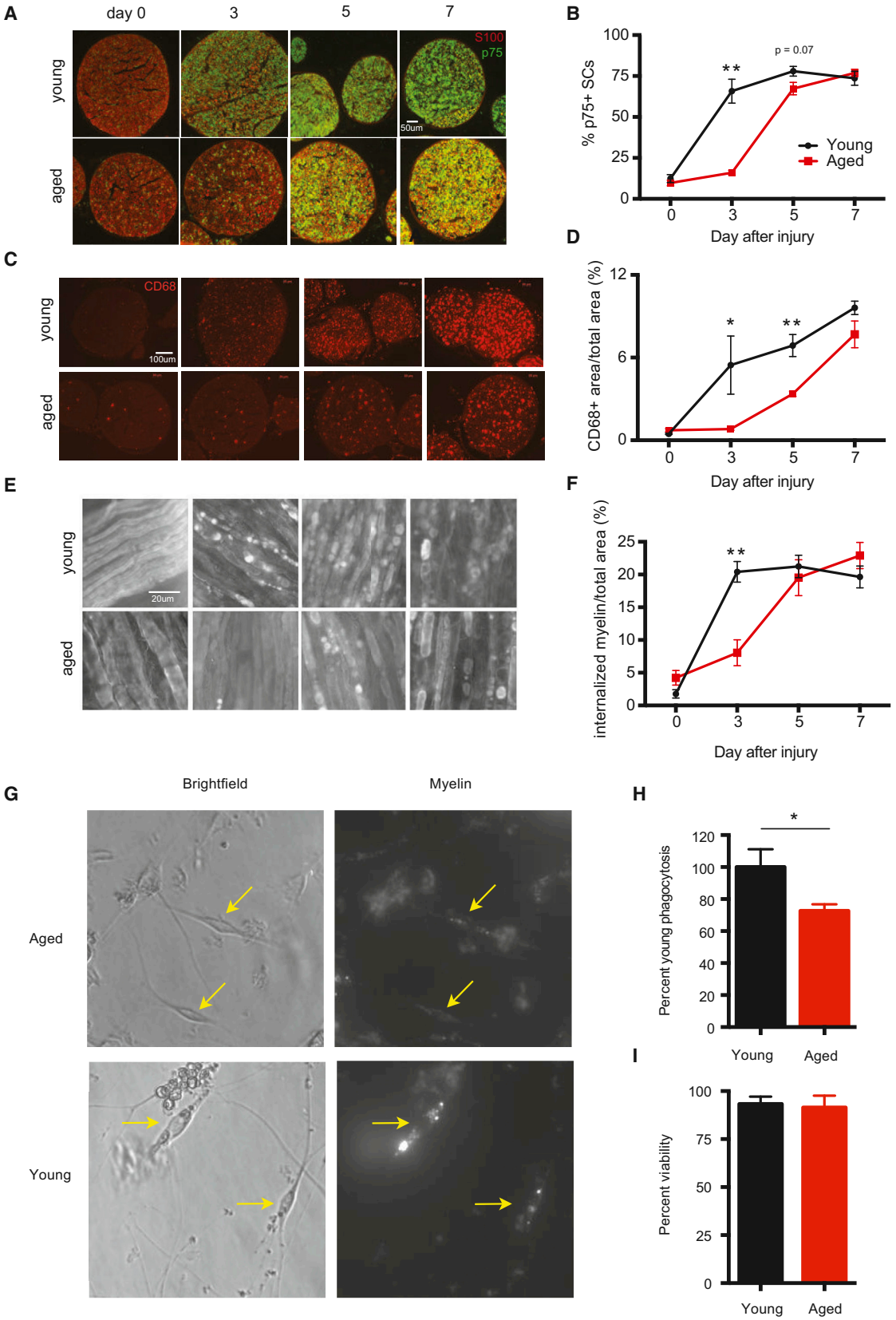

(legend on next page)

of the donor graft. The person who performed the surgeries never participated in the behavioral experiments.

Assessment of Motor Recovery by Toe-Spreading Test

Toe-spreading assay was performed as described previously (Ma et al., 2011). Briefly, mice were gently covered with a piece of cloth and lifted by the tail, uncovering the hind paws for clear observation, and the number of toes and extent of toe spreading was measured for the injured side and compared to the uninjured paw. Again, at least two separate investigators made independent assessments for each experiment. Nerve graft studies were completed blind to age of donor graft, and the surgeon did not participate in behavioral studies.

Microarray Analysis

Common pools of RNA were derived from ipsi- (injured) and contralateral (uninjured) L4 and L5 DRGs or ipsi- and contralateral sciatic nerves (1-cm-long segments distal to the site of injury), amplified, and hybridized to Illumina BeadChip arrays. All microarray experiments were conducted in biological triplicates, except for the DRGs from old naive animals, which were done in duplicate. Each replicate was composed of tissue from at least two separate animals. All analyses were carried out either in Excel or in GenePattern (http://www.genepattern.org) using the Multiplot module.

For pathway analyses, fold change differences were calculated between relative expression of each gene in young versus old mice 0 days and 4 days following injury. iPAGE was then applied on each of these fold change expression profiles to identify pathways that best explain the resulting differences in postinjury gene expression between young and old mice. The following methodology was developed by Goodarzi et al. and is more fully described in Goodarzi et al. (2009).

The continuous expression profiles were first quantized into 50 discreet, equally sized bins. Mutual information was then calculated between the expression profile and the pathway profile, a binary vector with n elements, one for each gene, indicating whether that gene belongs to the given GO or KEGG pathway. A nonparametric randomization statistical test was used to identify significantly informative pathways.

Quantification of Neurite Outgrowth

DRG sensory neurons were purified as described previously (Costigan et al., 1998). A total of 1,500–2,000 cells were plated on laminin and fixed 17 hr after plating (for naive) or 12 hr after plating (for preconditioned). Quantification was completed using Neuromath as described previously (Ma et al., 2011). Quantification was completed blind to age or condition and repeated three separate times.

Parabiosis

Parabiotic pairs were joined as previously described (Ruckh et al., 2012). All animals used for parabiotic pairings were male, from congenic strains to avoid immune rejection between the partners. Parabiotic pairings included isochronic-young pairs (2 young mice joined, each 8 weeks old), isochronic-old pairs (2 old mice joined, each 24 months old—all died), and heterochronic pairs (a young mouse joined to an old one, respective ages same as above).

Western Immunoblotting

Sciatic nerves were dissected from young and old mice at indicated days after sciatic nerve injury. Protein lysates from sciatic nerves were extracted in the presence of a protease cocktail tablet (Roche Diagnostics) using RIPA extraction buffer by homogenizer, and cell debris was removed by centrifugation (4°C, 15 min). Protein concentrations were determined by using BCA protein assay kit (Pierce). Equivalent amounts of protein were loaded and separated by SDS-PAGE and subsequently transferred to an Immobilon-P PVDF transfer membrane (Millipore). After washing in Tris-buffered saline (TBS) containing Tween 20, blots were blocked in 5% milk for 1 hr at room temperature (RT) and incubated with rabbit polyclonal antibodies against p-ERK (Cell Signaling, 1:500), total ERK (Sigma, 1:1,000), p-JNK (Cell Signaling, 1:500), total JNK (Cell Signaling, 1:500), ATF3 (Santa Cruz, 1:500), total c-Jun (Cell Signaling, 1:500), and a mouse monoclonal antibody against GAPDH (Chemicon, 1:2,000). Horseradish peroxidase (HRP)-conjugated secondary antibody (anti-rabbit, anti-mouse, Pierce, 1:5,000), an enhanced chemiluminescence (ECL) kit (Pierce), and autoradiography film (Genesee Scientific) were used following the manufacturer's protocol for signal detection.

Immunohistochemistry

Sciatic nerves were harvested distal to crush by perfusing mice with ice-cold PBS followed by cold 4% paraformaldehyde. Nerves were postfixed for 5 hr at 4°C. For myelin staining, epineurium was carefully removed and axon bundles were separated along natural divisions using forceps. Three to four small (~3 mm) segments of these bundles were cut at approximately the location of the nerve trifurcation. Segments were permeabilized in ice-cold methanol for 20 min and rinsed 3 × 10 min in blocking buffer (10% normal donkey serum, 1% Triton X-100 in PBS) at RT. For nerve bundle staining, briefly, segments were blocked in blocking buffer overnight at 4°C. Segments were incubated in primary antibodies: goat anti-p75 (Neuromics,1:500), rabbit anti-MBP (DAKO 1:100), diluted in blocking buffer at 4°C for 72 hr with rocking followed by 3 × 10 min washes at RT and 6 × 1 hr washes in blocking buffer at 4°C. Secondary antibodies (donkey anti-goat 488, donkey anti-rabbit 563, donkey anti-rat 633, Invitrogen) were diluted 1:1,000 in blocking buffer. Segments were incubated in secondary antibody for 48 hr at 4°C with rocking and rinsed as after primary antibody incubation followed by three clearing steps in 25%, 50%, and 75% glycerol, respectively, for 24 hr each at 4°C. Nerve bundles were mounted in glycerol-based Vectashield mounting media with DAPI.

For staining of sciatic nerve cross-sections, postfixed nerves were cryoprotected by sinking in 30% sucrose overnight. Frozen nerves were cryosectioned into 10 μm sections. Sections were permeabilized with ice-cold methanol for 10 min and blocked in blocking buffer (10% donkey serum, 0.2% Triton X-100) for 1 hr at RT followed by overnight incubation in primary antibody: goat anti-p75 (Neuromics, 1:500), rabbit anti-S100 (DAKO, 1:500), rat anti-CD68 (AbD serotec 1:1,000) at 4°C. Following 3 × 10 min PBS rinses at RT, slides were incubated overnight in secondary antibodies (Invitrogen, 1:1,000) at 4°C, rinsed 3 × 10 min in PBS, and mounted with Vectashield plus DAPI.

In Vitro Schwann Cell Phagocytosis Assay

Schwann cells were purified 3 days post sciatic nerve crush from 24-month-old and 8-week-old mice according to the methods described in Brosius Lutz (2014). Cells were plated at equal density into wells of a 96-well plate. The following day, cells in each well were rinsed once with DPBS and fed media supplemented with 5% FCS and 5 μl pH-sensitive dye (pHRODO)-labeled crude PNS myelin purified according to Larocca and Norton (2006). Myelin was quantified using BCA assay and used at a protein concentration of 800 μg/ml. After 2 hr incubation at 37°C, cells were trypsinized and resuspended in 30% FCS on ice. For flow cytometry analysis, data were collected in the Stanford Shared FACS Facility obtained using NIH S10 Shared

Figure 7. Functional Defects in Aged Schwann Cells

(A–C) Cross-sections and whole mounts of sciatic nerves from young and aged animals at days 0, 3, 5, and 7 after nerve crush injury stained with (A) S100 and p75, (B) CD68, and (C) MBP.

(D–F) Quantification of staining from (A)–(C). Mean ± SEM is plotted, n = 3–4 mice per group. $p < 0.05$ by two-way ANOVA for (D)–(F). *$p < 0.05$, **$p < 0.01$ with multiple t tests, Holm-Sidak correction. SCs were purified from the sciatic nerves of young and aged animals 3 days after sciatic nerve crush injury and incubated with myelin for 2 hr.

(G) Representative images of purified young and aged SCs with myelin (yellow arrows).

(H) Quantification of myelin contained within SCs by fluorescence-activated cell sorting (FACS) analysis.

(I) Cell viability as determined by DAPI staining. n = 3–4 per group. **$p < 0.01$ with unpaired t test.

Instrument Grant. Approximately 500 Schwann cells were analyzed per well using the facility's LSRII.UV. SCs to analyze were identified by forward scatter, side scatter, and viability (DAPI) gating. Mean PE-TR fluorescence (pHRODO) was calculated for each cell population.

Plastic Embedding and Light Microscopic Analysis of Sciatic Nerves

At 3 and 10 days after sciatic nerve crush injury, mice were intravascularly perfused with a solution containing 2% paraformaldehyde and 2% glutaraldehyde in PBS. The ipsilateral sciatic nerve was dissected out and kept in the fixative solution for 4 hr and next transferred to PBS. A 5–8 mm tissue segment distal to the crush injury site was removed from the sciatic nerve and immersed in a 1% osmium tetroxide solution (Ted Pella), dehydrated in a graded series of ethanol, and embedded in Epon resin (Ted Pella). Transverse sections at 0.5 μm thickness were stained with toluidine blue and coverslipped on glass slides and viewed in a Nikon E600 light microscope. For each nerve, the number of fibers showing myelin sheath preservation was determined.

Electron Microscopy of Sciatic Nerves

Ultrathin sections (60–70 nm thickness) were cut from plastic embedded sciatic nerve segments using an RMC Products PowerTome Ultramicrotome (Boeckeler Instruments). The ultrathin sections were collected on formvar-coated copper one-hole grids. The sections were counterstained with uranyl acetate and lead citrate and examined using a JEOL 100CX transmission electron microscope.

Quantification

Quantification was performed using National Institutes of Health ImageJ. Images were acquired using Zeiss Axio Imager M1 and Axiovision software. Images were analyzed blind.

Internalized Myelin Quantification. Image of nerve bundle was cropped to uniform size and MBP signal threshold was adjusted to reveal areas of intense MBP accumulation. Area occupied by MBP/area of nerve in cropped image was determined.

P75/S100 Quantification. For each cross-section, S100 and p75 signal threshold was adjusted to exclude background signal. A region of interest (ROI) was created based on the S100-positive area of the cross-section. This ROI was applied to the p75 image, and the percent of the ROI pixels positive for p75 was determined.

Thy1 YFP+ Fibers Quantification. Images of nerve sections from each distance from the suture site were taken at 10× magnification (at least three separate nerve images per animal per distance). The images were imported into ImageJ, converted to black and white, and converted into a binary image, and the number of "masks" was counted for each image. This was done in exactly the same procedure for each image, and all images were taken with the same exposure time.

Confocal images were obtained using a Zeiss LSM510 Meta inverted confocal microscope through the Stanford Neuroscience Microscopy Service, supported by NIH NS069375.

ACCESSION NUMBERS

The Gene Expression Omnibus accession numbers for the microarray profiling reported in this paper are GSE58982 and GSE59040 and will be made available July 30, 2014.

SUPPLEMENTAL INFORMATION

Supplemental Information includes five figures, three tables, and Supplemental Experimental Procedures and can be found with this article online at http://dx.doi.org/10.1016/j.neuron.2014.06.016.

ACKNOWLEDGMENTS

We thank David Roberson for help with figures, David Segal for assistance with behavioral experiments and setup, Olusegun Babaniyi for animal care, Giovanni Coppola for microarray data processing, David Parkinson and Xin-Peng Dun for advice on the whole-mount staining protocol, and Michael Costigan and Nadia Cohen for critical comments on the manuscript. We also thank Nick Andrews for advice on statistical analyses. This work was supported by the Dr. Miriam and Sheldon G. Adelson Medical Research Foundation (C.J.W., L.A.H., and B.B.), the Bertarelli Foundation (C.J.W.), NIH R01 NS038253 and P30 HD018655 (C.J.W.), NIH RO1 AG033053 and UO1 HL100402 (A.J.W.), NIH NRSA F31 AG042227-02 (M.W.P.), S10RR027431-01 (B.B), NIH NS069375 (B.B.), NIH T32 HD007249 Developmental and Neonatal Biology Training Program (A.B.L.), and the Stanford MSTP and School of Medicine (A.B.L.). A.J.W. is an Early Career Scientist of the Howard Hughes Medical Institute.

Accepted: June 12, 2014
Published: July 16, 2014

REFERENCES

Arthur-Farraj, P.J., Latouche, M., Wilton, D.K., Quintes, S., Chabrol, E., Banerjee, A., Woodhoo, A., Jenkins, B., Rahman, M., Turmaine, M., et al. (2012). c-Jun reprograms Schwann cells of injured nerves to generate a repair cell essential for regeneration. Neuron *75*, 633–647.

Barrette, B., Hébert, M.A., Filali, M., Lafortune, K., Vallières, N., Gowing, G., Julien, J.P., and Lacroix, S. (2008). Requirement of myeloid cells for axon regeneration. J. Neurosci. *28*, 9363–9376.

Bonilla, I.E., Tanabe, K., and Strittmatter, S.M. (2002). Small proline-rich repeat protein 1A is expressed by axotomized neurons and promotes axonal outgrowth. J. Neurosci. *22*, 1303–1315.

Brosius Lutz, A. (2014). Purification of Schwann cells from the neonatal and injured adult mouse peripheral nerve. In Purifying and Culturing Neural Cells: A Laboratory Manual, B.A. Barres and B. Stevens, eds. (Cold Spring Harbor: Cold Spring Harbor Laboratory Press), pp. 177–188.

Brosius Lutz, A., and Barres, B.A. (2014). Contrasting the glial response to axon injury in the central and peripheral nervous systems. Dev. Cell *28*, 7–17.

Chen, Z.L., Yu, W.M., and Strickland, S. (2007). Peripheral regeneration. Annu. Rev. Neurosci. *30*, 209–233.

Cho, D.Y., Mold, J.W., and Roberts, M. (2006). Further investigation of the negative association between hypertension and peripheral neuropathy in the elderly: an Oklahoma Physicians Resource/Research Network (OKPRN) study. J. Am. Board Fam. Med. *19*, 240–250.

Chong, M.S., Reynolds, M.L., Irwin, N., Coggeshall, R.E., Emson, P.C., Benowitz, L.I., and Woolf, C.J. (1994). GAP-43 expression in primary sensory neurons following central axotomy. J. Neurosci. *14*, 4375–4384.

Costigan, M., Mannion, R.J., Kendall, G., Lewis, S.E., Campagna, J.A., Coggeshall, R.E., Meridith-Middleton, J., Tate, S., and Woolf, C.J. (1998). Heat shock protein 27: developmental regulation and expression after peripheral nerve injury. J. Neurosci. *18*, 5891–5900.

Goodarzi, H., Elemento, O., and Tavazoie, S. (2009). Revealing global regulatory perturbations across human cancers. Mol. Cell *36*, 900–911.

Graciarena, M., Dambly-Chaudière, C., and Ghysen, A. (2014). Dynamics of axonal regeneration in adult and aging zebrafish reveal the promoting effect of a first lesion. Proc. Natl. Acad. Sci. USA *111*, 1610–1615.

Kang, H., and Lichtman, J.W. (2013). Motor axon regeneration and muscle reinnervation in young adult and aged animals. J. Neurosci. *33*, 19480–19491.

Larocca, J.N., and Norton, W.T. (2006). Isolation of myelin. Curr. Protoc. Cell Biol. http://dx.doi.org/10.1002/0471143030.cb0325s33.

Lundborg, G., and Rosén, B. (2001). Sensory relearning after nerve repair. Lancet *358*, 809–810.

Ma, C.H., Omura, T., Cobos, E.J., Latrémolière, A., Ghasemlou, N., Brenner, G.J., van Veen, E., Barrett, L., Sawada, T., Gao, F., et al. (2011). Accelerating axonal growth promotes motor recovery after peripheral nerve injury in mice. J. Clin. Invest. *121*, 4332–4347.

McKerracher, L., David, S., Jackson, D.L., Kottis, V., Dunn, R.J., and Braun, P.E. (1994). Identification of myelin-associated glycoprotein as a major myelin-derived inhibitor of neurite growth. Neuron *13*, 805–811.

Mirsky, R., Woodhoo, A., Parkinson, D.B., Arthur-Farraj, P., Bhaskaran, A., and Jessen, K.R. (2008). Novel signals controlling embryonic Schwann cell development, myelination and dedifferentiation. J. Peripher. Nerv. Syst. *13*, 122–135.

Nagano, A. (1998). Treatment of brachial plexus injury. J. Orthop. Sci. *3*, 71–80.

Napoli, I., Noon, L.A., Ribeiro, S., Kerai, A.P., Parrinello, S., Rosenberg, L.H., Collins, M.J., Harrisingh, M.C., White, I.J., Woodhoo, A., and Lloyd, A.C. (2012). A central role for the ERK-signaling pathway in controlling Schwann cell plasticity and peripheral nerve regeneration in vivo. Neuron *73*, 729–742.

Pestronk, A., Drachman, D.B., and Griffin, J.W. (1980). Effects of aging on nerve sprouting and regeneration. Exp. Neurol. *70*, 65–82.

Ruckh, J.M., Zhao, J.W., Shadrach, J.L., van Wijngaarden, P., Rao, T.N., Wagers, A.J., and Franklin, R.J. (2012). Rejuvenation of regeneration in the aging central nervous system. Cell Stem Cell *10*, 96–103.

Seijffers, R., Mills, C.D., and Woolf, C.J. (2007). ATF3 increases the intrinsic growth state of DRG neurons to enhance peripheral nerve regeneration. J. Neurosci. *27*, 7911–7920.

Shen, S., Sandoval, J., Swiss, V.A., Li, J., Dupree, J., Franklin, R.J., and Casaccia-Bonnefil, P. (2008). Age-dependent epigenetic control of differentiation inhibitors is critical for remyelination efficiency. Nat. Neurosci. *11*, 1024–1034.

Tanaka, K., and Webster, H.D. (1991). Myelinated fiber regeneration after crush injury is retarded in sciatic nerves of aging mice. J. Comp. Neurol. *308*, 180–187.

Vaughan, D.W. (1992). Effects of advancing age on peripheral nerve regeneration. J. Comp. Neurol. *323*, 219–237.

Verdú, E., Ceballos, D., Vilches, J.J., and Navarro, X. (2000). Influence of aging on peripheral nerve function and regeneration. J. Peripher. Nerv. Syst. *5*, 191–208.

Woodhall, B., ed. (1956). Peripheral Nerve Regeneration: A Follow-up Study of 3,656 World War II Injuries (Washington, D.C.: U.S. Government Printing Office).

Zou, Y., Chiu, H., Zinovyeva, A., Ambros, V., Chuang, C.F., and Chang, C. (2013). Developmental decline in neuronal regeneration by the progressive change of two intrinsic timers. Science *340*, 372–376.